

Improved performance of Au nanocrystal nonvolatile memory by N_2-plasma treatment on HfO_2blocking layer

Chen Wang(王尘), Yi-Hong Xu(许怡红), Song-Yan Chen(陈松岩), Cheng Li(李成), Jian-Yuan Wang(汪建元), Wei Huang(黄巍), Hong-Kai Lai(赖虹凯), Rong-Rong Guo(郭榕榕)
Citation: Chin. Phys. B . 2018, 27(6): 067303. **doi:** 10.1088/1674-1056/27/6/067303

Journal homepage: http://cpb.iphy.ac.cn; http://iopscience.iop.org/cpb

What follows is a list of articles you may be interested in

Stress-induced leakage current characteristics of PMOS fabricated by a new multi-deposition multi-annealing technique with full gate last process

Yanrong Wang(王艳蓉), Hong Yang(杨红), Hao Xu(徐昊), Weichun Luo(罗维春), Luwei Qi(祁路伟), Shuxiang Zhang(张淑祥), Wenwu Wang(王文武), Jiang Yan(闫江), Huilong Zhu(朱慧珑), Chao Zhao(赵超), Dapeng Chen(陈大鹏), Tianchun Ye(叶甜春)
Chin. Phys. B . 2017, 26(8): 087304. **doi:** 10.1088/1674-1056/26/8/087304

High holding voltage SCR for robust electrostatic discharge protection

Zhao Qi(齐钊), Ming Qiao(乔明), Yitao He(何逸涛), Bo Zhang(张波)
Chin. Phys. B . 2017, 26(7): 077304. **doi:** 10.1088/1674-1056/26/7/077304

Analytical capacitance model for 14 nm FinFET considering dual-*k* spacer

Fang-Lin Zheng(郑芳林), Cheng-Sheng Liu(刘程晟), Jia-Qi Ren(任佳琪), Yan-Ling Shi(石艳玲), Ya-Bin Sun(孙亚宾), Xiao-Jin Li(李小进)
Chin. Phys. B . 2017, 26(7): 077303. **doi:** 10.1088/1674-1056/26/7/077303

Improvement of reverse blocking performance in vertical power MOSFETs with Schottky-drain-connected semisuperjunctions

Wei Mao(毛维), Hai-Yong Wang(王海永), Xiao-Fei Wang(王晓飞), Ming Du(杜鸣), Jin-Feng Zhang(张金凤), Xue-Feng Zheng(郑雪峰), Chong Wang(王冲), Xiao-Hua Ma(马晓华), Jin-Cheng Zhang(张进成), Yue Hao(郝跃)
Chin. Phys. B . 2017, 26(4): 047306. **doi:** 10.1088/1674-1056/26/4/047306

An analytical model for nanowire junctionless SOI FinFETs with considering three-dimensional coupling effect

Fan-Yu Liu(刘凡宇), Heng-Zhu Liu(刘衡竹), Bi-Wei Liu(刘必慰), Yu-Feng Guo(郭宇峰)
Chin. Phys. B . 2016, 25(4): 047305. **doi:** 10.1088/1674-1056/25/4/047305

Improved performance of Au nanocrystal nonvolatile memory by N_2-plasma treatment on HfO_2 blocking layer*

Chen Wang(王尘)[1,†], Yi-Hong Xu(许怡红)[2], Song-Yan Chen(陈松岩)[3], Cheng Li(李成)[3], Jian-Yuan Wang(汪建元)[3], Wei Huang(黄巍)[3], Hong-Kai Lai(赖虹凯)[3], and Rong-Rong Guo(郭榕榕)[1]

[1] *Fujian Provincial Key Laboratory of Optoelectronic Technology and Devices, School of Opto-electronic and Communiction Engineering, Xiamen University of Technology, Xiamen* 361024, *China*

[2] *Xiamen Institute of Technology, Xiamen* 361024, *China*

[3] *Department of Physics, Semiconductor Photonics Research Center, Xiamen University, Xiamen* 361005, *China*

(Received 22 January 2018; revised manuscript received 21 March 2018; published online 10 May 2018)

The N_2-plasma treatment on a HfO_2 blocking layer of Au nanocrystal nonvolatile memory without any post annealing is investigated. The electrical characteristics of the MOS capacitor with structure of Al–TaN/HfO_2/SiO_2/p-Si are also characterized. After N_2-plasma treatment, the nitrogen atoms are incorporated into HfO_2 film and may passivate the oxygen vacancy states. The surface roughness of HfO_2 film can also be reduced. Those improvements of HfO_2 film lead to a smaller hysteresis and lower leakage current density of the MOS capacitor. The N_2-plasma is introduced into Au nanocrystal (NC) nonvolatile memory to treat the HfO_2 blocking layer. For the N_2-plasma treated device, it shows a better retention characteristic and is twice as large in the memory window than that for the no N_2-plasma treated device. It can be concluded that the N_2-plasma treatment method can be applied to future nonvolatile memory applications.

Keywords: Au nanocrystal nonvolatile memory, N_2-plasma, HfO_2 dielectric film.

PACS: 73.40.Qv, 61.46.Hk, 52.77.–j, 77.55.–g **DOI:** 10.1088/1674-1056/27/6/067303

1. Introduction

Nanocrystal memory employing distributed nanodots as storage elements instead of the continuous polysilicon floating gate in conventional flash memory structures has been a promising candidate for replacing conventional nonvolatile memory (NVM). Due to discrete storage nodes, continuous charge leakage caused by localized oxide defects will not happen. This allows the more aggressive scaling of the tunnel oxide to achieve lower operating voltages and faster write/erase speeds for a high performance NVM. Compared with the semiconductor counterparts, metal NCs exhibit several advantages, such as a wide range of available work functions, higher density of states around the Fermi level, stronger coupling with the conduction channel, and smaller energy perturbation due to carrier confinement.[1,2] Especially, the noble metals do not oxidize nor react with the surrounding dielectric layers.[3] For these reasons, Au NCs receive a lot of attention. In addition, the high dielectric constant (high-k, $k > 3.9$) materials instead of SiO_2 ($k \sim 3.9$) as the dielectric layers could also be utilized to enhance the memory performance. The use of the high-k materials as a blocking layer makes the voltage drop across the blocking layer lower, and more electric field will fall on the tunneling oxide,[3] thus reducing the write/erase voltage of the device. Furthermore, high-k blocking layers offer a smaller equivalent oxide thickness (EOT) with relatively thick film, which is important for leakage suppression and device scaling. Among the high-k candidates, HfO_2 has been spotlighted due to its high dielectric constant (~ 25), large band gap (~ 5.6 eV), and thermodynamic stability.[4,5] However, it was reported that oxygen vacancy (V_O) is dominant over an intrinsic defect, and is also considered to present a high concentration in HfO_2.[4,6,7] The V_O levels in HfO_2 are located at about 1.2 eV below the bottom of the conduction bands, which has a crucial relation with electron leakage current[8,9] and will degrade the performance of the device.

Recently, nitrogen incorporation has been investigated in ultrathin HfO_2 dielectric film to passivate the oxygen vacancy states. Several approaches, such as high temperature annealing in NH_3 ambient,[10] *in situ* nitrogen incorporation using ALD by adding nitrogen plasma[11] and the reactive sputtering method followed by a reoxidation anneal[12] have been reported. These studies showed that the nitrogen incorporation provides some improvement in device characteristics, but there still remain some drawbacks. High temperature annealing may cause HfO_2 to crystallize for its crystallization temperature is rather low (~ 400 °C). Grain boundaries in crystallized gate dielectric films may act as oxygen or dopant diffusion paths, leading to a significant increase in leakage current and making EOT scaling problematic. The NH_3 is toxic gas, and it can also introduce hydrogen-related traps (–H, –OH, and N–H), which will cause a degradation in the device stability. Moreover, post-deposition annealing may also affect the NCs

*Project supported by the High Level Talent Project of Xiamen University of Technology, China (Grant Nos. YKJ16012R and YKJ16016R) and the National Natural Science Foundation of China (Grant No. 51702271).

†Corresponding author. E-mail: chenwang@xmut.edu.cn

© 2018 Chinese Physical Society and IOP Publishing Ltd

in the memory.

In this paper, a simple method of incorporating nitrogen into HfO_2 by post-N_2 plasma without any post annealing is investigated. N_2-plasma treatment proves to be a feasible and simple fabrication process with low thermal budget to improve the electrical properties of the HfO_2 dielectric. The N_2-plasma treatment is also introduced into Au nanocrystal memory with HfO_2 blocking layers resulting in larger memory windows and better retention characteristics than that without N_2-plasma treatment. It is indicated that the simple method of N_2-plasma treatment promises to be applied to future nonvolatile memory.

2. Method

A p-type Si(100) wafer with a resistivity of 1 Ω·cm–10 Ω·cm was used and cleaned with the standard RCA process, followed by a dry oxidation process at 900 °C to form a ∼ 5-nm-thick SiO_2 layer as a tunnel oxide. Subsequently, a thin layer of Au was deposited on the tunnel oxide using radio frequency (RF) magnetron sputtering at a relatively low power of 40 W. The Au NCs were formed after rapid thermal annealing at 600 °C for 60 s in N_2 ambient. Afterwards, a 21-nm-thick HfO_2 layer was deposited onto the tunnel oxide by electron-beam evaporation as the blocking oxide layer. Then, the N_2-plasma treatment was performed on the as-deposited HfO_2 under an optimized plasma processing condition (90 W for 10 min with 40-sccm N_2) by using reactive ion etching. Finally, the sputter-deposited 50-nm TaN and 300-nm Al gate electrodes were both patterned on the HfO_2 film by a shadow mask, while the 300-nm Al was sputtered as the back electrode. For comparison, the Au nanocrystal memory capacitor without N_2-plasma treatment was also fabricated. Moreover, the Al–TaN/HfO_2/SiO_2/p–Si MOS capacitors without Au NCs were also fabricated by using the same processing steps to investigate the properties of the HfO_2 films before and after N_2-plasma treatment.

The nitrogen incorporation into HfO_2 film was confirmed by x-ray photoelectron spectroscopy (XPS). The HfO_2 morphology was determined by image processing of atomic force microscopy (AFM). High-resolution cross-sectional transmission electron microscopy (HRTEM) analyses were performed to investigate the structure of the Au nanocrystal memory capacitor with N_2-plasma treatment. Capacitance–voltage (C–V) and current–voltage (I–V) characteristics were determined by using a Keithley 4200 semiconductor parameter analyzer with an HP4284 *LCR* meter. The C–V curves were measured at an applied frequency of 1 MHz.

3. Results and discussion

Prior to the XPS analyses, about 2-nm-thick surfaces of the samples are removed by 4-keV Ar ion bombardment, thereby removing contaminants from the surfaces. The XPS depth profiles of the sample of ∼ 21-nm-thick HfO_2 film on the SiO_2/p-Si substrate with and without N_2-plasma treatment are shown in Fig. 1. From Fig. 1(a), we can see that no N 1s peak can be detected from the sample without N_2-plasma treatment. However, an obvious N 1s peak near 396.3 eV is detected for the sample after N_2-plasma treatment in an optimized condition, showing the formation of N–Hf bonds.[12] The intensity of the N 1s peak is strongest in the middle area, and decreases with the depth increasing to the top area or decreasing to the bottom area. Figure 1(b) shows the XPS of the Hf 4f peak from HfO_2 film with and without N_2-plasma treatment in the middle area. The well-resolved transition metal core level doublet spectrum (Hf $4f_{7/2}$ and Hf $4f_{5/2}$) of the sample corresponds to as-deposited HfO_2 while sample after N_2-plasma treatment has a relatively poorly resolved spectrum. The spectrum acquired from the as-deposited HfO_2 shows an Hf $4f_{7/2}$ peak at a binding energy of 17.1 eV, which corresponds to the Hf–O bond in bulk HfO_2[13] as shown in Fig. 1(b). The main peak of the sample with N_2-plasma treatment shifts to a lower binding energy of about 16.9 eV due to the presence of nitrogen in the film.[14] The modeling associated with achieving a very good fit with the measured spectrum for the sample with N_2-plasma in Fig. 1(b) indicates the contribution of Hf–N bond-related peaks at 15.8 eV, 17.8 eV in Hf 4f to the resultant spectrum.[15] The results clearly indicate that a trace quantity of N element is introduced into the HfO_2 thin film and an oxygen vacancy might be occupied by an N atom after N_2-plasma treatment.[9,12,14]

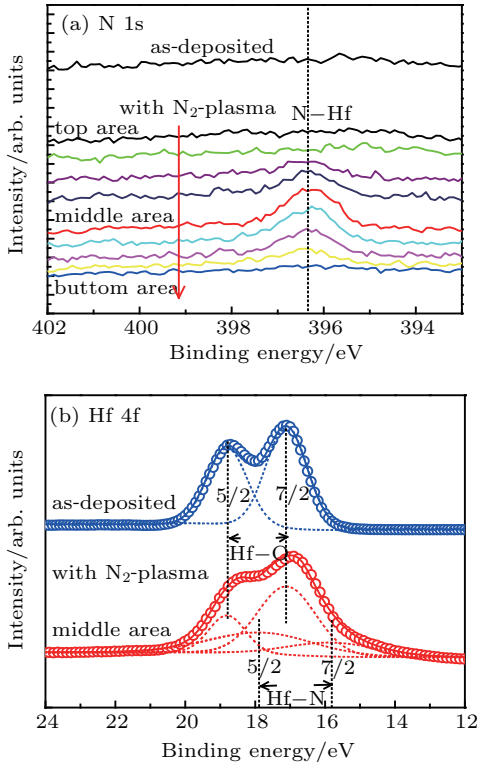


Fig. 1. (color online) XPS spectra of (a) N 1s and (b) Hf 4f from HfO_2 film deposited by e-beam in the cases with and without N_2-plasma treatment.

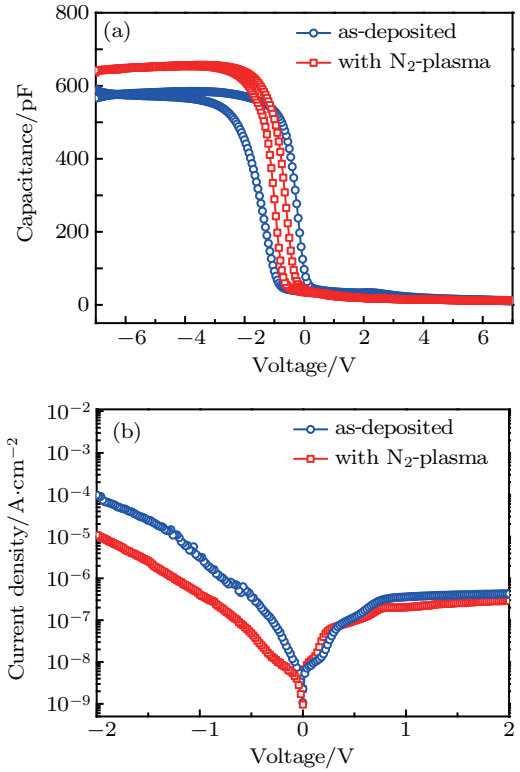


Fig. 2. (color online) (a) Capacitance-voltage and (b) current-voltage characteristics of MOS capacitors with and without N_2-plasma treatment on HfO_2 film.

Figure 2(a) shows the *C*–*V* measurement results of the Al–TaN/HfO_2/SiO_2/p-Si MOS capacitors with and without N_2-plasma treatment on HfO_2 film, respectively. The gate voltage is swept from accumulation to inversion and back to check the magnitude of hysteresis. The capacitor without N_2-plasma treatment exhibits a large hysteresis of about 1.3 V at ±6 V, suggesting a higher density of charge trapping centers. In contrast, hysteresis is significantly reduced to 0.2 V in the plasma-nitrided HfO_2 MOS capacitor in the same sweeping range. It indicates that the N_2-plasma treatment on HfO_2 film can effectively reduce the density of charge trapping centers such as oxygen vacancies, which results in hysteresis. In addition, the larger accumulation capacitance of the capacitor after N_2-plasma treatment suggests the improved quality of HfO_2 and better electrical properties of the MOS capacitor. The leakage current characteristics of the MOS capacitors with and without N_2-plasma treatment are shown in Fig. 2(b). The leakage current density of gate injection for the capacitor with N_2-plasma treatment is about 4.1×10^{-7} A/cm^2 at −1-V applied voltage, which is one order of magnitude lower than that without N_2-plasma (about 3.1×10^{-6} A/cm^2). The leakage current characteristic is improved by using the N_2-plasma process, which is believed to be due to the fact that the incorporated nitrogen atoms can occupy the oxygen vacancies, reduce the number of traps, and hinder the conduction of leakage electrons,[8,9] which is in accordance with the result of the *C*–*V* measurement. After N_2-plasma treatment, the surface quality of HfO_2 can also be improved, which is confirmed by analyzing the surface morphology of the HfO_2 film on SiO_2/p-Si by AFM as shown in Fig. 3. As we can see, the root-mean-square (RMS) surface roughness of the as-deposited sample is about 0.45 nm, but it greatly reduces to 0.14 nm after N_2-plasma treatment. It was reported that the surface roughness can cause an additional potential across the insulating film, which increases the average electric field inside the film, resulting in the increase of the leakage current density.[16] As a consequence, the smooth surface of HfO_2 after N_2-plasma treatment may also contribute to the reduction of leakage current density.

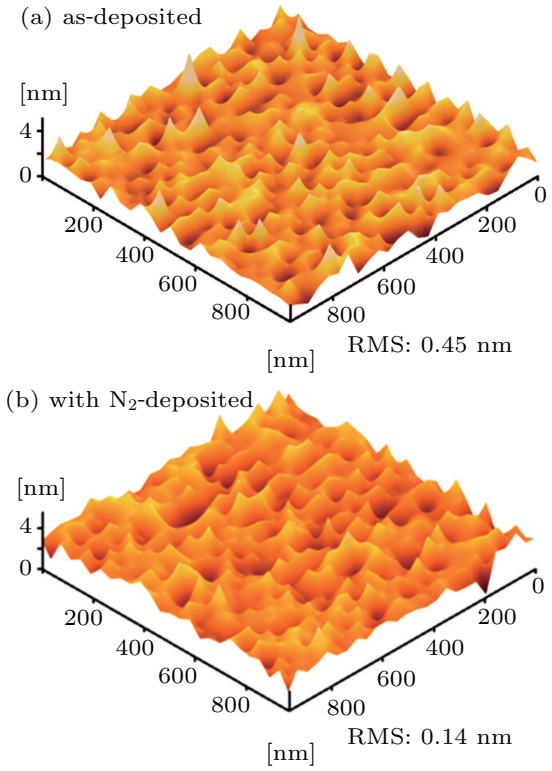


Fig. 3. (color online) Tapping mode AFM 3D pictures of the HfO_2 film on SiO_2/p-Si with and without N_2-plasma treatment. The surface roughness is also estimated from the RMS value.

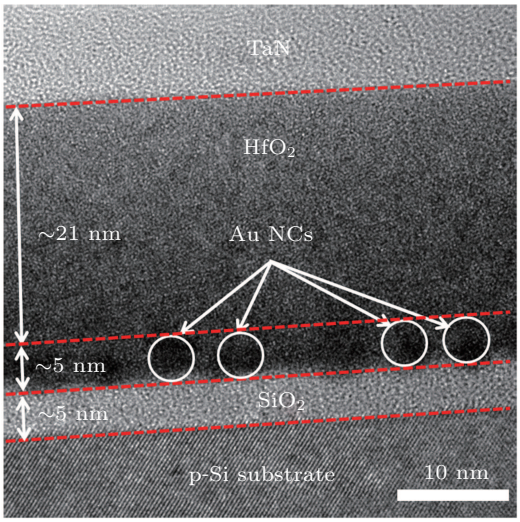


Fig. 4. (color online) Cross-sectional HRTEM micrograph of Au NCs memory capacitor with N_2-plasma treatment.

Figure 4 shows the cross-sectional high-resolution transmission electron microscopy (HRTEM) micrograph of Au nanocrystal memory capacitor with N_2-plasma treatment. The Au NCs formed on the 5-nm thermal SiO_2 are covered with a 21-nm HfO_2 layer. The NC density is approximately 8.4×10^{11} cm^{-2}, wherein the mean size is about 5 nm. The HRTEM of the memory capacitor without N_2-plasma treatment shows a similar NC distribution and size (not shown here). It indicates that the post-N_2-plasma treatment rarely affects the formation of Au NC.

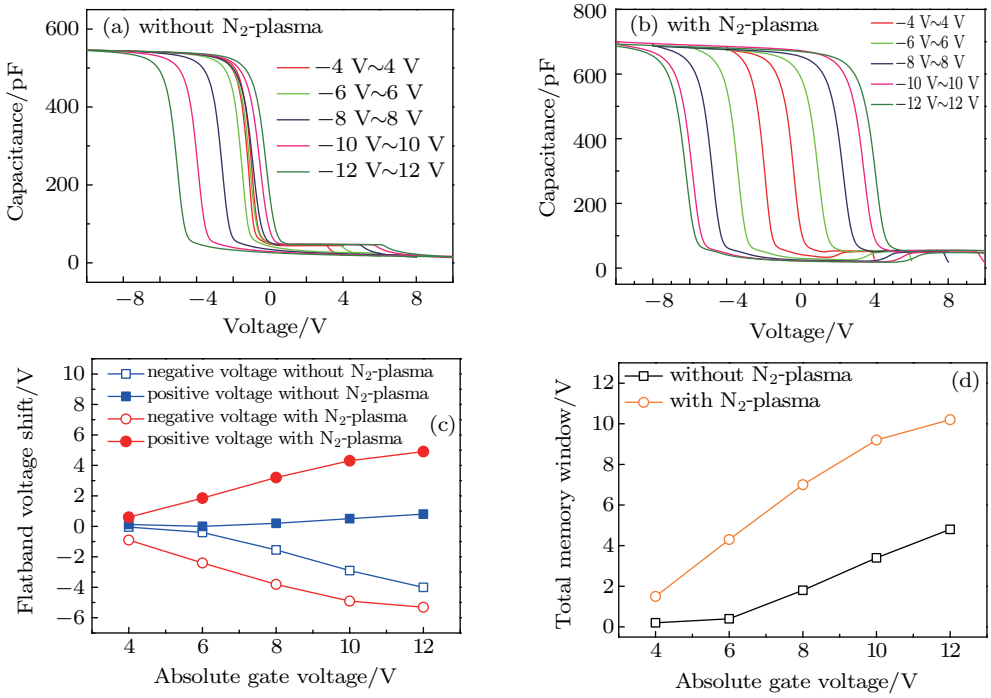


Fig. 5. (color online) Normalized *C*–*V* characteristics for different voltage sweeps of Au NCs memory (a) with and (b) without N_2-plasma treatment on HfO_2 blocking layer. (c) Evolution of flat-band voltage shift and (d) total memory window as a function of absolute gate bias.

Figures 5(a) and 5(b) show the *C*–*V* hysteresis after bidirectional sweeps in various voltage ranges, which compares with the memory characteristics of the two kinds of Au nanocrystal memory capacitors with and without N_2-plasma treatment on the HfO_2 blocking layer. The flat-band voltage shift and memory window are extracted and shown in Figs. 5(c) and 5(d), respectively. As we can see, the memory windows of the devices all increase almost linearly with applied voltage due to the observed flat-band voltage shifts at both bias polarities, which confirms successive charging by electrons (positive bias) and holes (negative bias).[17,18] Nevertheless, the flat-band voltage shifts at either bias polarity of the memory capacitor with N_2-plasma treatment are higher throughout, leading to a much higher memory window and demonstrating the larger storage capacity. A 10.2-V memory window is obtained for the memory capacitor with N_2-plasma treatment at ±12-V sweep. Compared with other reported results,[3,19,20] the memory window here is not the best result. However, it is twice as large as that without N_2-plasma treatment in the same applied voltage range, which is a big improvement. According to Fig. 2(a), negligible hysteresis windows are measured for the MOS capacitor with N_2-plasma treatment, indicating that almost all the charges are stored in the Au NCs.[20] On the contrary, for the memory capacitor without N_2-plasma treatment, except Au NCs, part of charge can also be trapped in the HfO_2 blocking layer, which can contribute to the oxygen vacancy existing in HfO_2. The charge storage density can be calculated from the relation $N = \Delta V_{FB} C/q$,[3,18] where C is the capacitance density and ΔV_{FB} is the flat-band voltage shift. On the basis of this relation, the negative and positive charge densities trapped in the memory capacitor with N_2-plasma treatment at ±12 V are estimated at 1.7×10^{13}/cm^2 and 1.8×10^{13}/cm^2 respectively, while for the memory capacitor without N_2-plasma treatment are 2.1×10^{12}/cm^2 and 1.1×10^{13}/cm^2 respectively. The charge densities of the latter are much lower, although part of charges can also be trapped in the HfO_2 film. It confirms that the significant leakage passages exist in the HfO_2 film without N_2-plasma treatment. Charges stored in Au NCs may easily leak out via the trapping centers.[21] Moreover, after N_2-plasma treatment, the oxide quality surrounding the Au NCs can be improved and de-trapping via traps is suppressed, which is consistent with the results as shown in Fig. 2. Saturation of the flat-band voltage shifts and memory window set in when the applied voltage range reaches to ±12 V for the N_2-plasma treated memory capacitor, which could be attributed to the Coulomb blockade effect originating from the field induced by the stored charge.[22] It should be noted that the memory window compared with other reported results may not be the largest in this study. However, the goal of this work

is to clarify the significant improvement of the NVM performance by the simple method of N_2-plasma treatment on the HfO_2 blocking layer. In addition, further optimization, such as the mean size and number density of Au NCs, can be carried out to improve the performances of these memory devices.

The retention characteristics of the memory capacitors with and without N_2-plasma at room temperature, extrapolated to 10 years, are shown in Fig. 6. The capacitors are programmed first with a drive voltage of +7 V for 1 s. Next, the *C*–*V* is measured with an applied voltage of +7 V to −0.5 V and the flat band voltage is extracted. The memory capacitor is then erased under −7 V for 1 s and the *C*–*V* characteristics are measured at different time intervals in a voltage range from −7 V to 0.5 V. The *C*–*V* measurements are repeated at different time intervals up to 10^5 s for both cases. Extrapolation to 10 years yields charge losses of about 19% and 32% for the memory capacitors with and without N_2-plasma, respectively. The retention properties of the sample with N_2 plasma treatment are superior. In general, if more charges are stored in the traps rather than in the nanocrystals, the more serious degradation of memory window can be expected. As we can see from Fig. 2, the smaller hysteresis and the lower leakage current of the MOS capacitor fulfilled by using the N_2-plasma process suggest much less traps existing in HfO_2. Therefore, the improved retention characteristic is believed to be due to the fact that the N_2 plasma treatment can repair defects and improve the surrounding HfO_2 quality of Au nanocrystals.

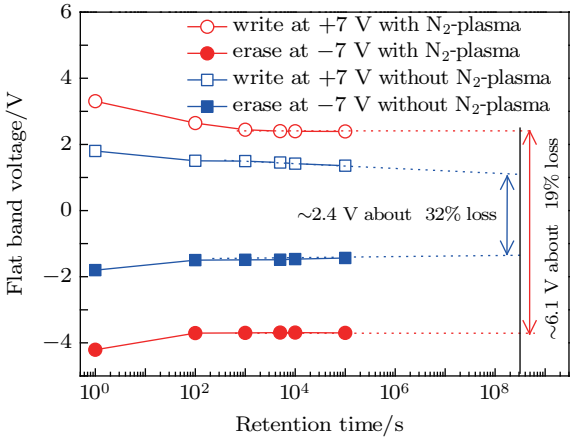


Fig. 6. (color online) Retention characteristics of memory capacitors with and without N_2-plasma at room temperature.

4. Conclusions

In this paper, we have demonstrated the N_2-plasma treatment on the HfO_2 blocking layer of Au nanocrystal nonvolatile memory. After N_2-plasma treatment, the nitrogen atoms are incorporated into HfO_2 film and might passivate the oxygen vacancy states, leading to the reduction of traps. The surface roughness of HfO_2 film can also be reduced after N_2-plasma treatment. Those improvements of HfO_2 film lead to a smaller hysteresis and lower leakage current density of the MOS capacitor. The N_2-plasma is introduced into the Au nanocrystal nonvolatile memory to treat the HfO_2 blocking layer. For the N_2-plasma treated memory, it shows a larger memory window and better retention characteristics. Therefore, Au nanocrystal memory with suitable nitrogen incorporation promise to be used in future nonvolatile memory devices.

References

[1] Liu Z, Lee C, Narayanan V and Pei G 2002 *IEEE Trans. Electron Dev.* **49** 1606
[2] Chan K C, Lee P F and Dai J Y 2008 *Appl. Phys. Lett.* **92** 223105
[3] Mikhelashvili V, Meyler B, Yoffis S, Salzman J, Garbrecht M, Cohen-Hyams T, Kaplan W D and Eisenstein G 2009 *Appl. Phys. Lett.* **95** 023104
[4] Xiong Y, Tu H, Du J, Ji M G, Zhang X and Wang L 2010 *Appl. Phys. Lett.* **97** 012901
[5] Zhu W J, Ma T P, Zafar S and Tamagawa T 2002 *IEEE Electron Dev. Lett.* **23** 597
[6] Gavartin J L, Ramo D M, Shluger A L, Bersuker G and Lee B 2006 *Appl. Phys. Lett.* **89** 082908
[7] Xiong K, Robertson J, Gibson M C and Clark S 2005 *Appl. Phys. Lett.* **87** 183505
[8] Umezawa N, Shiraishi K, Ohno T, Watanabe H, Chikyow T, Torii K, Yamabe K, Yamada K, Kitajima H and Arikado T 2005 *Appl. Phys. Lett.* **86** 143507
[9] Xiong K, Robertson J and Clark S J 2006 *J. Appl. Phys.* **99** 044105
[10] Akbar M S, Gopalan S, Cho H J, Onishi K, Choi R, Nieh R, Kang C, Kim Y, Han J and Krishnan S 2003 *Appl. Phys. Lett.* **82** 1757
[11] Maeng W J and Kim H 2007 *Appl. Phys. Lett.* **91** 092901
[12] Kang C S, Cho H J, Onishi K, Nieh R, Choi R, Gopalan S, Krishnan S, Han J H and Lee J C 2002 *Appl. Phys. Lett.* **81** 2593
[13] Renault O, Samour D, Damlencourt J F, Blin D, Martin F, Marthon S, Barrett N and and Besson P 2002 *Appl. Phys. Lett.* **81** 3627.
[14] Wang L, Xue K, Xu J B, Huang A and Chu P K 2007 *Appl. Phys. Lett.* **90** 122901
[15] Maeng W, Gu G H, Park C, Lee K, Lee T and Kim H 2009 *J. Electrochem. Soc.* **156** G109
[16] Zhao Y P, Wang G C, Lu T M, Palasantzas G and De Hosson J T M 1999 *Phys. Rev. B* **60** 9157
[17] Lee P F and Dai J Y 2010 *Nanotechnology* **21** 295706
[18] Xu Z, Zhu C, Huo Z, Cui Y, Wang Y, Li F and Liu M 2012 *Appl. Phys. Lett.* **100** 203509
[19] Dufourcq J and Bodnar S 2008 *Appl. Phys. Lett.* **92** 073102
[20] Mikhelashvili V, Meyler B, Yofis S, Shneider Y, Zeidler A, Garbrecht M, Cohen-Hyams T, Kaplan W, Lisiansky M and Roizin Y 2011 *Appl. Phys. Lett.* **98** 212902
[21] Chang T C, Jian F Y, Chen S C and Tsai Y T 2011 *Mater. Today* **14** 608
[22] She M and King T J 2003 *IEEE Trans. Electron Dev.* **50** 1934